

Supplementary Data

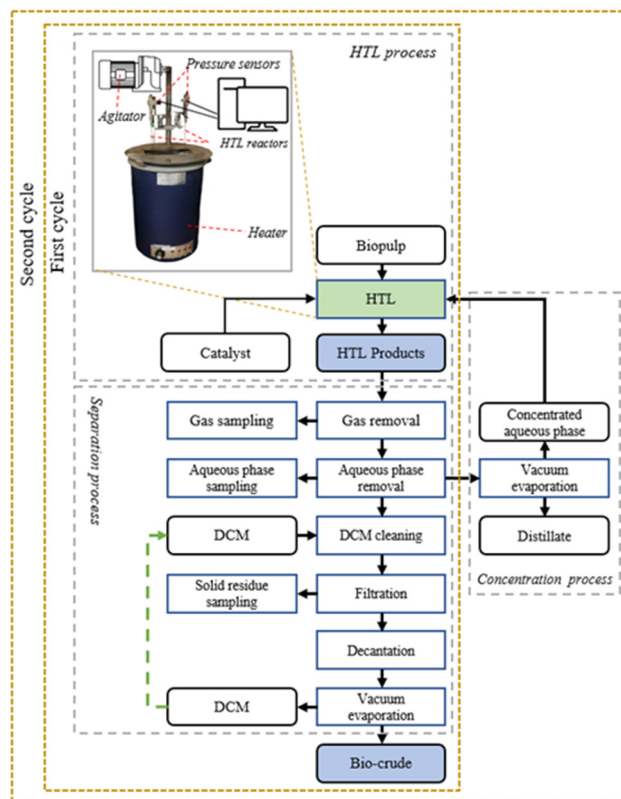
# Bio-crude production improvement during hydrothermal liquefaction of biopulp by simultaneous application of alkali catalysts and aqueous phase recirculation

Komeil Kohansal<sup>a</sup>, Kamaldeep Sharma<sup>a</sup>, Saqib Sohail Toor<sup>a</sup>, Eliana Lozano Sanchez<sup>a</sup>, Joscha Zimmermann<sup>b</sup>, Lasse Aistrup Rosendahl<sup>a</sup>, Thomas Helmer Pedersen<sup>\*a</sup>

<sup>a</sup> Department of Energy Technology, Aalborg University, Pontoppidanstræde 111, 9220 Aalborg, Denmark;

<sup>b</sup> Institute of Catalysis Research and Technology (IKFT), Karlsruhe Institute of Technology (KIT), Hermann-von-Helmholtz-Platz 1, 76344 Eggenstein-Leopoldshafen, Germany;

\* Correspondence: thp@aabu.dk; Tel: +45-28291679



Citation: Kohansal, K.; Sharma, K.; Toor, S.S.; Sanchez, E.L.; Zimmermann, J.; Aistrup Rosendahl, L.; Pedersen, T.H. Bio-Crude Production Improvement during Hydrothermal Liquefaction of Biopulp by Simultaneous Application of Alkali Catalysts and Aqueous Phase Recirculation. *Energies* 2021, 14, 4492. <https://doi.org/10.3390/en14154492>

**Figure S1.** The schematic plot of HTL, concentration, and separation processes.

**Publisher's Note:** MDPI stays neutral with regard to jurisdictional claims in published maps and institutional affiliations.



**Copyright:** © 2021 by the authors. Submitted for possible open access publication under the terms and conditions of the Creative Commons Attribution (CC BY) license (<http://creativecommons.org/licenses/by/4.0/>).

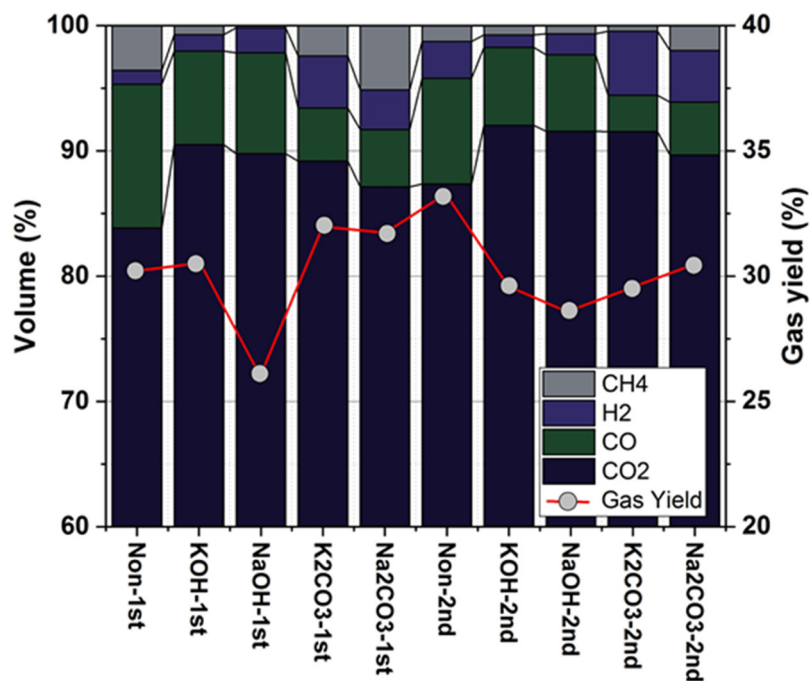


Figure S2. Gas yield and composition.

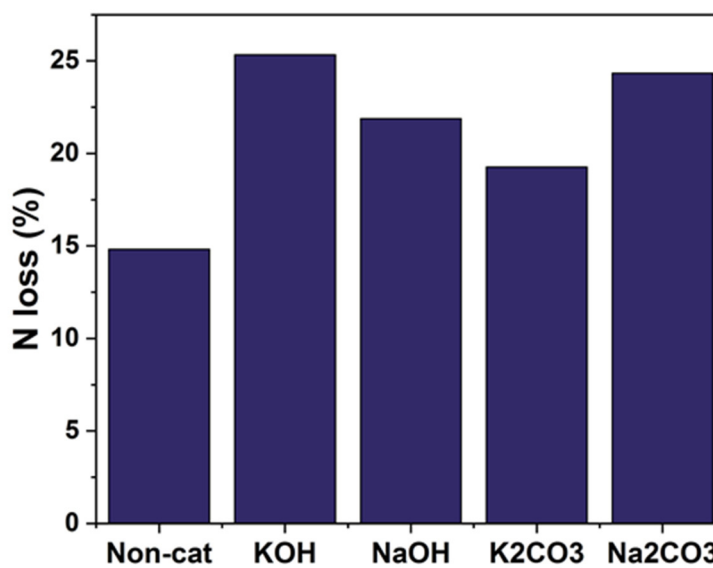


Figure S3. Total nitrogen loss during concentration of aqueous phase.

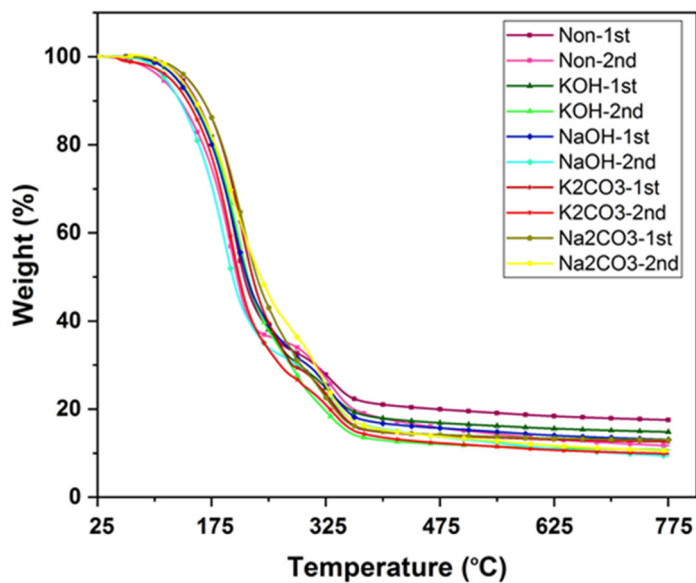


Figure S4. Thermogravimetric curves of the bio-crudes obtained in different experiments.

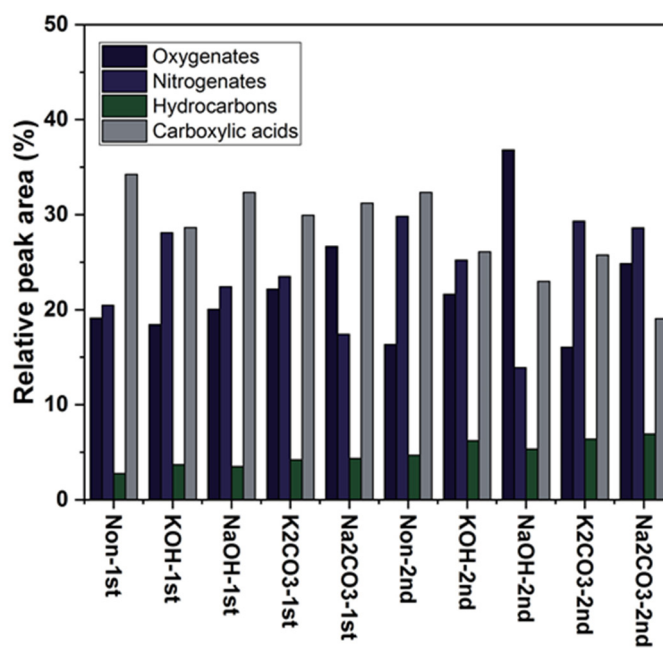
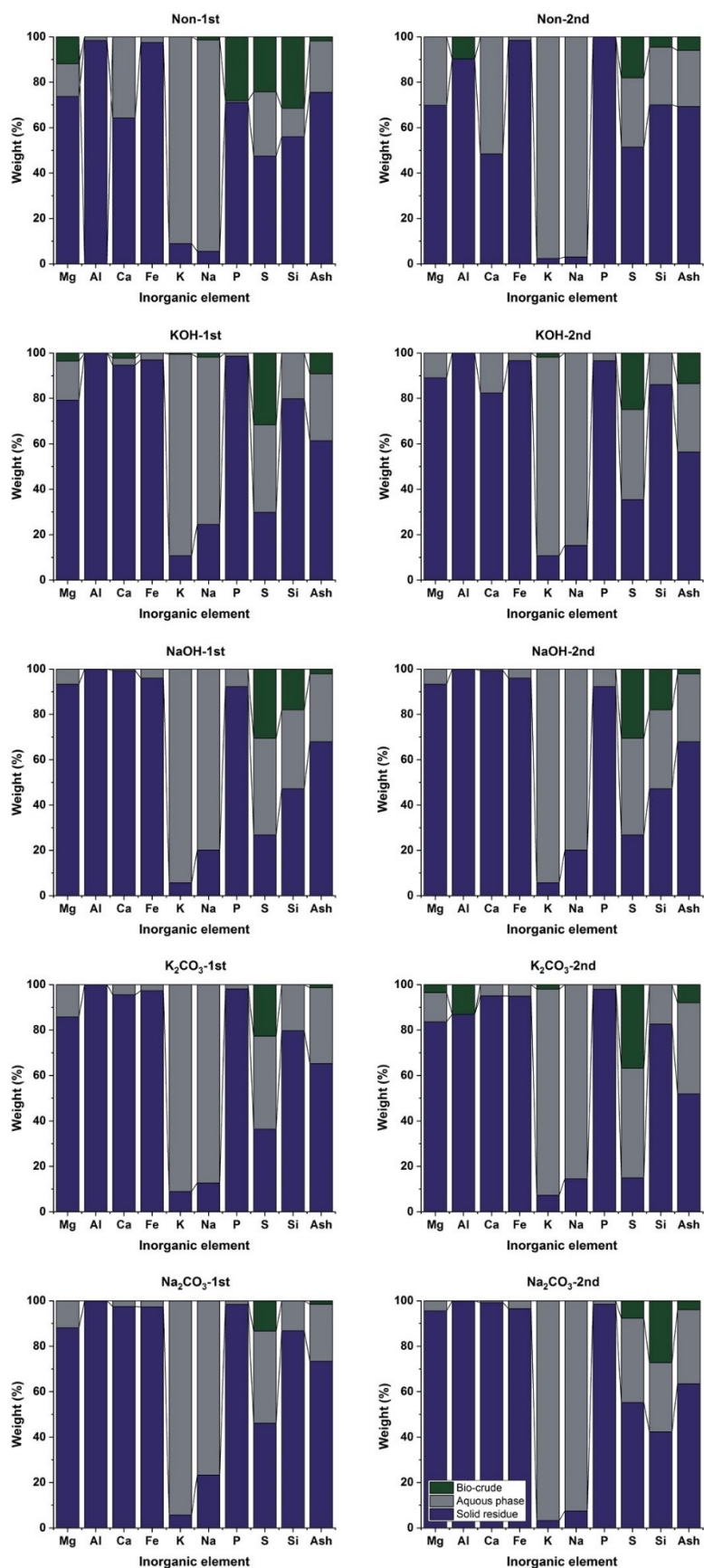


Figure S5. Categorized GC-MS analysis results for the bio-crude samples achieved from recirculation set of experiments.

**Table S1.** The major organic compounds (relative peak area >1 %) identified in bio-crude obtained at first and second cycles non-catalytic and K<sub>2</sub>-CO<sub>3</sub> catalytic experiments.

No.	RT	Compound	Peak Area (%)			
			Non-1st	Non-2nd	K <sub>2</sub> CO <sub>3</sub> -1st	K <sub>2</sub> CO <sub>3</sub> -2nd
1	11.39	1,5,5-Trimethyl-6-methylene-cyclohexene	ND*	1.32	ND	1.78
2	12.05	Undecane	ND	1.81	1.02	1.34
3	13.32	1-Ethyl-2-pyrrolidinone	ND	1.56	ND	ND
4	14.37	3-Cyclohexene-1-carboxaldehyde, 1,3,4-trimethyl	ND	ND	1.11	1.27
5	19.30	Dodecanoic acid	1.02	ND	ND	ND
6	21.51	Tetradecanoic acid	1.34	ND	ND	ND
7	23.57	n-Hexadecanoic acid	7.74	5.11	7.42	4.59
8	23.78	Hexadecanoic acid, ethyl ester	1.78	1.48	2.87	2.01
9	24.45	Dodecanoic acid, 3-hydroxy	1.12	1.04	1.0	ND
10	25.31	Vaccenic acid	23.19	20.31	19.77	15.14
11	25.41	9-Octadecenoic acid (Z)-, methyl ester	6.62	4.55	8.26	6.16
12	25.67	9-Octadecenamide, (Z)	3.13	2.17	2.26	1.90
13	25.94	N-Methyldodecanamide	2.76	3.33	1.34	4.89
14	26.28	N,N-Dimethyldodecanamide	4.10	8.60	3.5	7.56
15	27.21	9-Octadecenamide, (Z)-	3.70	4.61	3.92	4.86
16	27.76	9-Octadecenamide, N,N-dimethyl	4.90	7.41	4.06	5.01
17	28.18	Oxiraneoctanoic acid, 3-octyl-, cis	ND	1.12	1.16	ND
18	28.52	Ethyl iso-allocholate	3.1	1.30	3.15	1.45
19	28.91	n-Dodecanoylpyrrolidine	ND	1.89	ND	2.10
20	29.64	Oleic diethanolamide	1.02	2.04	1.20	ND

\*ND: Not detected



**Figure S6.** Inorganic elements distribution during HTL process.